

Mechanism for clogging of microchannels

Hans M. Wyss,¹ Daniel L. Blair,¹ Jeffrey F. Morris,² Howard A. Stone,³ and David A. Weitz¹

¹*Department of Physics & DEAS, Harvard University, Cambridge, Massachusetts 02138, USA*

²*Levich Institute at the City University of New York, New York, New York 10031, USA*

³*DEAS, Harvard University, Cambridge, Massachusetts 02138, USA*

(Received 18 April 2006; published 11 December 2006)

We investigate clogging of microchannels at the single-pore level using microfluidic devices as model porous media. The process of clogging is studied at low volume fractions and high flow rates, a technologically important regime. We show that clogging is independent of particle flow rate and volume fraction, indicating that collective effects do not play an important role. Instead, the average number of particles that can pass through a pore before it clogs scales with the ratio of pore to particle size. We present a simple model that accounts for the data.

DOI: [10.1103/PhysRevE.74.061402](https://doi.org/10.1103/PhysRevE.74.061402)

PACS number(s): 82.70.-y, 47.55.Kf, 47.56.+r, 47.61.Jd

The extraction of solids from fluids is a common and important process in industry and technology; deep-bed filtration in oil recovery, ground water treatment, catalysis, and liquid chromatography all depend on the capture of solid particles inside a porous medium. However, a serious limitation to the performance of all filters is ultimately the clogging of the porous medium. Clogging can also lead to catastrophic results in technologies which rely on the complete suppression of any kind of blockage, such as ink-jet printing or any microfluidic system where particles are present either intentionally or unintentionally in the form of dust or other contaminants. However, despite their importance, the physical mechanisms that lead to clogging of porous media are still not well understood. Physically, filters are porous media with a distribution of pore sizes that determines the smallest filtrate to be removed from suspension. The simplest possible picture of clogging is one of pure size exclusion, where blockage events occur only if particles enter a pore that is smaller than their own diameter. However, in many instances clogging is observed even when the pores are much larger than the suspended particles.

The process of clogging is exceptionally complicated and not well understood. Model descriptions of clogging often focus on different length scales than do typical experimental investigations. However, a sound theoretical description of clogging ultimately must be based on an understanding of the blockage mechanism at the level of a single pore. Unfortunately, experimental studies typically focus on macroscopic clogging in realistic porous materials such as packed grains [1,2], or porous membranes [3]. Although these experiments provide important insight into the dynamics of clogging in the pore network as a whole, clogging on the single-pore level cannot be accessed. Without experimental data on clogging at the single-pore level, a full interpretation of clogging phenomena in macroscopic porous media will remain elusive. Thus, experimental measurements of clogging at the single-pore scale are essential.

In this article, we report experimental results of filtration and clogging at the single pore level. We observe that the formation of clogs is determined solely by a critical number of particles that flow through single pores irrespective of both flow rate and particle volume fraction. Moreover, we show that this critical number scales in an unexpected way

with the ratio of the pore to particle size and we present a simple model that correctly accounts for this scaling.

We flow particle suspensions through a microfluidic device that consists of a single wide channel followed by an array of parallel, narrow channels [see Fig. 1(a)]; this design allows us to investigate a large number of clogging events simultaneously. Each channel consists of a set of constrictions along their length. The height of the channel is held constant and is the same as that of the large incoming channel. We control the flow rate of the suspension in the channels by setting the pressure difference of the fluid across the channels. This approach ensures that the flow rate in any given channel does not depend on the state of the other channels. Clogging events are independently characterized under identical conditions, allowing us to acquire statistical information about the random clogging process. The ratio of the pore to particle size is varied over an order of magnitude: the width of the pores is varied over tens of micrometers and the particle diameter is on the order of micrometers. Controlled and well-defined pore structures are produced by fabricating poly-(dimethylsiloxane) (PDMS) microfluidic devices using soft lithography [4,5]. Our devices have four PDMS walls and are fabricated without plasma activation to ensure the surface wetting properties remain constant in time [6]. We use aqueous suspensions of uniform polystyrene spheres that are electrosterically stabilized by sulfate and carboxyl surface groups (IDC).

We use digital video microscopy to record movies of the microfluidic channels and measure the dynamics of clogging at the single-pore level. The typical transit time of a particle through the entire microfluidic device is ~ 0.1 s. Thus, at standard video rates, we cannot image individual particles passing through pores. Instead, we capture images of the average particle concentration. The intensity of a point in the image reflects the average local number concentration of particles; the darker the region, the higher the local particle concentration. A typical experimental image is shown in Fig. 1(a). The gray regions on the left correspond to a volume fraction of $\phi = 4 \times 10^{-2}$, while the lightest regions are either PDMS walls or pure water. The regions that appear darkest are areas of highly concentrated particles near a clog. A time series of the clogging process for three channels is shown in Fig. 1(b). The darkest shades of gray (red online) indicate

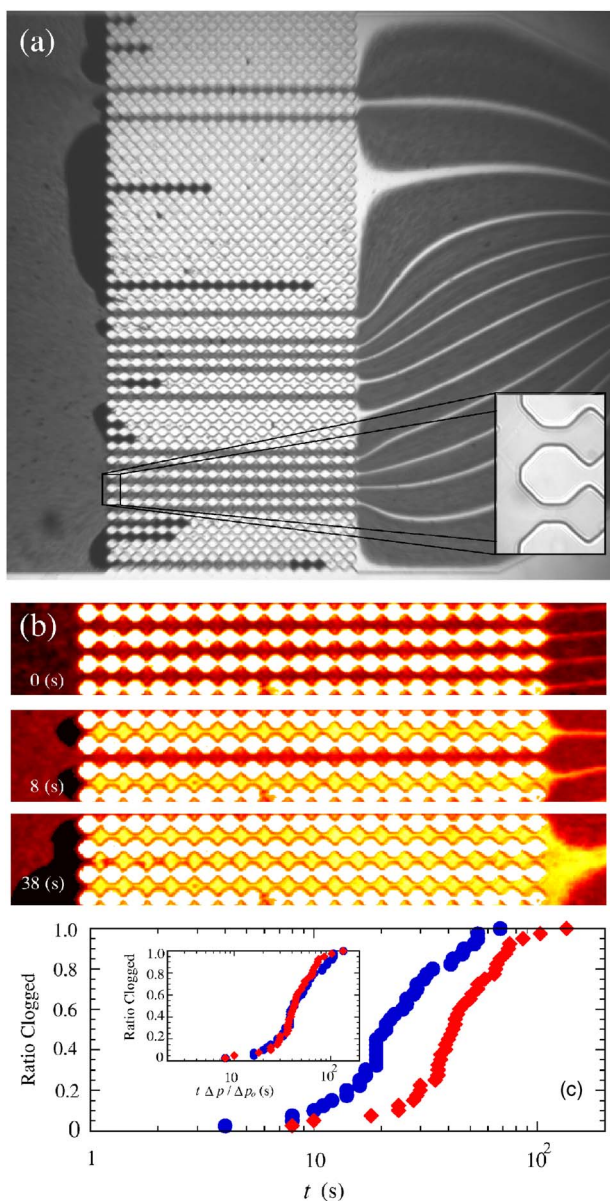


FIG. 1. (Color online) (a) Microscope image of a microfluidic device during a clogging experiment. A particle suspension of volume fraction $\phi=4 \times 10^{-2}$ is pumped from left to right through a series of channels in the device. The pressure difference between inlet and outlet is held constant at $\Delta p=2$ psi; the total length of the channels is 1.2 mm. The particle diameter is $D=2.9 \mu\text{m}$; the height of the device is $H=25 \mu\text{m}$. Inset: close-up of the channel exit zone; the smallest width at the bottleneck of each channel is $W=20 \mu\text{m}$. (b) Close-up of three channels in the device as a time series, $t=0$ s, 8 s, 38 s. (c) Dependence on applied pressure for the same geometry. The ratio of clogged channels as a function of time at different applied pressures. $\Delta p=2$ psi (red diamonds, results of experiment shown on top); $\Delta p=4$ psi (blue circles). Inset: plot of the same data with time normalized by the relative pressure difference $\Delta p/\Delta p_0$ ($\Delta p_0=2$ psi).

regions where particles are densely packed, whereas particle-free fluid appears light gray (yellow online); the channel side walls are shown in white. At $t=0$ s the areas inside the channels appear evenly gray, demonstrating that particles are homogeneously distributed. At $t=8$ s two channels have be-

come clogged at their inlets and the central channel is still open to particles and fluid. In the last frame, $t=38$ s, all three channels are clogged and a region of densely packed particles spans their inlets. After each clogging event, the porosity of the clog remains nonzero and therefore fluid continues to flow. As a consequence, a “filter cake” of packed particles builds up on the upstream side of the clog location.

To quantify the clogging process, we measure the ratio of clogged to open channels as a function of time [see Fig. 1(c)]. For these data, we fix the pore geometry and volume fraction. The diamonds correspond to the experiment displayed in Fig. 1(a). At higher pressures clogging occurs faster, as shown by the circles. We normalize the data by the ratio of the applied pressure to the lowest applied pressure, $\Delta p/\Delta p_0$, where $\Delta p_0=2.0$ pounds per square inch (psi). This rescaling eliminates the dependence on flow rate, as shown in Fig. 1(c), inset, indicating that a fixed volume of fluid must pass through the pore prior to clogging.

One possible mechanism for clogging is the random occurrence of a local particle concentration large enough to result in a physical blocking of pores [7] or arch formation within a channel [8], even though the typical number of particles in a pore is very small; for example, at $\phi=0.01$, there are typically only ~ 4 particles passing through a pore of cross section $W \times H=25 \times 20 \mu\text{m}^2$ at any given moment. In a stable suspension, fluctuations in the particle concentration, at length scales comparable to pore sizes, will be determined by Poisson statistics. As the volume fraction is increased, it becomes more probable that a concentration fluctuation will be large enough to fill a pore with particles, thus blocking it. As a consequence, clogging should be strongly dependent on ϕ .

To test the dependence on such local concentration fluctuations, we vary the volume fraction and measure the change in the average clogging time t^* from the curves in Fig. 1(c), while holding all other experimental parameters fixed. We normalize t^* by the relative applied pressure and plot the result as a function of ϕ (in Fig. 2). As ϕ varies between 4×10^{-4} and 4×10^{-2} , t^* varies by two orders of magnitude from seconds to hours. Within experimental error, t^* is not only inversely proportional to the flow rate Q of suspension flowing through a channel, but also on the particle volume fraction ϕ :

$$t^* \propto \frac{1}{Q\phi}. \quad (1)$$

While the clogging time is strongly ϕ dependent, the effects of fluctuations will be most apparent in the total number of particles that must flow through a channel prior to clogging,

$$N^* \simeq t^* Q \phi / V_p. \quad (2)$$

Due to the inverse dependence of t^* on Q and ϕ , N^* is independent of ϕ . Thus, fluctuations due to Poisson statistics cannot describe the clogging mechanism since the marked insensitivity of N^* to both ϕ and Q indicates that pore clogging must be a single-particle effect.

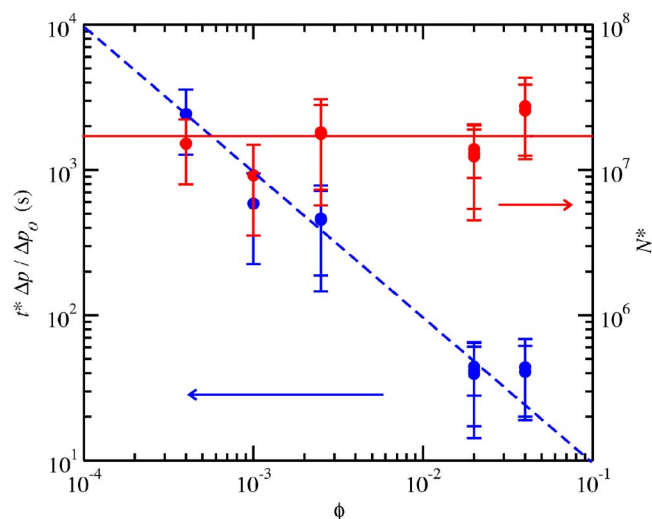


FIG. 2. (Color online) Dependence of the average clogging time t^* and the number N^* of particles required to clog a channel on the particle volume fraction ϕ . Clogging times of experiments taken at pressure differences $\Delta p \neq \Delta p_0 = 2$ psi are normalized by the relative pressure difference $\Delta p / \Delta p_0$. The dotted line is a power-law fit to the data with a resulting slope of -1 . The solid line is a constant value.

To elucidate the mechanism of clogging, we vary W/D , the ratio of the constriction width W , to the particle diameter D , while keeping the channel height fixed at $H \approx 25 \mu\text{m}$. We observe a very strong dependence of N^* on W/D , as shown in Fig. 3. The dependence is well described by a power law, as shown by the solid line which is a fit to the data, $N^* \propto (W/D)^m$, with an exponent $m = 4 \pm 0.1$.

To interpret this scaling, we propose a model based on successive particle buildup through irreversible sticking events near the constriction. We assume that a sticking event is determined by the initial streamline on which a particle is traveling prior to reaching any constriction. The fluid follows streamlines, which must be compressed at constrictions. Far away from a constriction, particles follow the same streamlines; however, at constrictions solid particles are forced to move relative to the fluid. This movement must result from physical forces, such as viscous lubrication and electrostatic surface forces, which are repulsive and drive particles away from the sidewalls. Therefore, for particles to stick at constrictions, their distance of approach to the sidewall must be comparable to the length scale where attractive surface forces dominate and some fraction of these particles will interact strongly with the sidewalls and stick irreversibly. We assume that all particles initially found on streamlines that pass within a characteristic distance $\epsilon \ll D$ from the sidewall will stick irreversibly to the wall; this region is shown schematically within the inset of Fig. 3(a). The probability of sticking for any particle is thus given by the fraction of streamlines that pass through the region associated with irreversible sticking events. Consequently, the sticking probability of a particle is given by the ratio of the flow rate Q_{stick} through the sticking region to the total flow rate Q_{total} ,

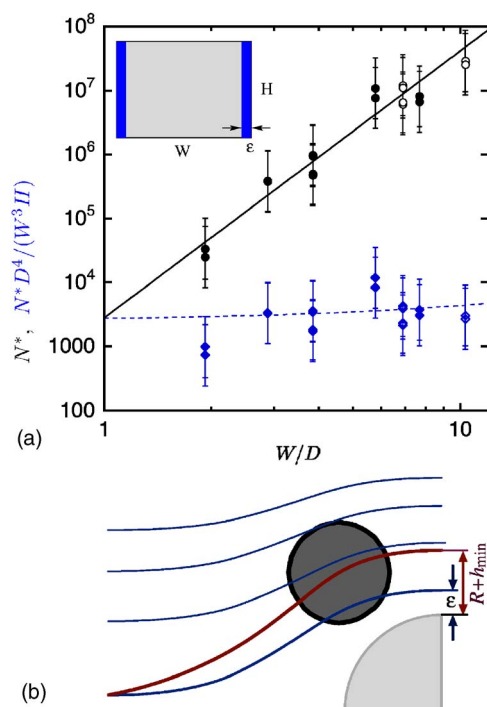


FIG. 3. (Color online) (a) Number of particles, N^* , that pass through a pore before clogging as a function of W/D (circles). The same data rescaled according to the prediction of our simple model (diamonds). Solid symbols: $D = 5.2 \mu\text{m}$. Open symbols: $D = 2.9 \mu\text{m}$. Inset: schematic pore cross section. Shown in blue are the “sticking areas” of width ϵ and height H . (b) Schematic illustration of fluid streamlines (blue) and a particle trajectory (red) at a constriction.

$$p_{\text{stick}} = \frac{Q_{\text{stick}}}{Q_{\text{total}}} = \frac{\epsilon H v_{\text{stick}}}{WH v_{\text{total}}}, \quad (3)$$

where $v_{\text{stick}}/v_{\text{total}}$ is the ratio of the average velocity in the sticking region to that in the overall constriction. With each sticking event the effective channel area decreases, while the width of the sticking area, ϵ , remains approximately the same. After n sticking events have already occurred, the sticking probability $p_{\text{stick}}(n)$ becomes

$$p_{\text{stick}}(n) = \frac{\alpha DH}{WH - nD^2} \frac{v_{\text{stick}}(n)}{v_{\text{total}}(n)}, \quad (4)$$

where $\alpha = \epsilon/D$; the additional nD^2 term accounts for the reduction in the total cross-sectional area through the addition of particles stuck to the wall. The number of particles that pass through the pore before complete clogging occurs is then $N^* = \sum_{n=0}^N 1/p_{\text{stick}}(n)$, where $N = WH/D^2$ is the number of particles needed to fill the channel cross section. Assuming a parabolic velocity profile in the channel the velocity ratio becomes $v_{\text{stick}}(n)/v_{\text{total}}(n) \approx 2\alpha DH/(WH - nD^2)$, where we assume that αD is small compared to the effective width of the channel $W_{\text{eff}}(n) \approx (WH - nD^2)/H$. Therefore, the average number of particles that must flow through a channel constriction before clogging occurs is

$$N^* \approx \frac{1}{2} \sum_{n=0}^N \frac{(WH - nD^2)^2}{\alpha^2 D^2 H^2} \approx \frac{W^3 H}{6\alpha^2 D^4}. \quad (5)$$

We plot $N^* D^4 / W^3 H$ as a function of W/D in Fig. 3(a); within experimental error, this quantity is independent of the ratio between pore and particle size, as illustrated by a linear fit to the data, shown by the dotted line.

The trajectory of a particle, shown schematically in Fig. 3(b), is determined by the balance of the repulsive forces and the drag force towards the wall, induced by the fluid. In our model, the occurrence of a sticking event is determined only by the initial streamline a particle is traveling on prior to any constriction. We assume that there exists a limiting fluid streamline [9,10] that is located a distance $\epsilon = \alpha D$ from the sidewall. Thus, the critical distance of minimum approach should correspond to a length that is comparable to the attractive well of the interaction potential that stabilizes particles against aggregation. An order-of-magnitude estimate of forces acting on a particle shows that the dominant repulsive mechanism is viscous lubrication. This suggests that particle trajectories are independent of fluid flow rate, as the dominant repulsive and attractive forces are both proportional to fluid velocity. This is also in agreement with the observed flow-rate independence of the clogging.

Remarkably, ϵ is determined directly from our macroscopic experimental data [see Fig. 3(a)]. By rescaling the data in Fig. 3(a), we obtain $\epsilon \approx 10$ nm, a length scale not directly discernible in our measurements. However, this length scale is comparable to the typical width of an electrostatic double layer at low ionic concentrations.

A consequence of our model is that the time scale for clogging should depend sensitively on the length scale of the repulsive interactions. To test this, we perform experiments in the presence of salt (NaCl), over a broad concentration range from 10^{-3} to 0.1 mol/L (see Fig. 4). The addition of counter-ions screens the surface charge, eventually leading to spontaneous aggregation of the colloidal particles at salt concentrations >0.1 mol/L. However, at salt concentrations be-

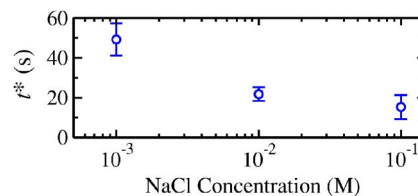


FIG. 4. (Color online) Characteristic clogging time scale t^* of single pores versus the NaCl concentration. The error bars represent the standard deviation of t^* .

low this value, we observe distinctly faster clogging dynamics with increasing salt concentration; both the average clogging time t^* and the corresponding length scale ϵ increased by a factor of 3 within the range of salt concentrations studied. Thus, the characteristic length scale of particle capture, ϵ , which is independent of the flow rate, is closely linked to the forces that regulate particle stability.

Using a simple macroscopic technique for tracking the blockage times of microfluidic channels, we characterize the physical processes that govern single-pore clogging dynamics at the nanometer scale. The dynamics of clogging and the length scale ϵ may provide an alternate measure of the stability of particle suspensions. Our clogging picture is not limited to the dependence on colloidal interaction forces. It captures the dependence of clogging dynamics on the relevant experimental parameters, thus providing a surprisingly general picture for the dynamics of clogging processes at the single-pore level. This single-pore clogging mechanism is thus an essential first step in understanding and predicting blockage of real porous materials that consist of interconnected pore networks.

We thank A. Ajdari, E. Dufresne, and E. Weeks for discussions and Halliburton, the NSF (Grant No. DMR-0602684), and the Harvard MRSEC (Grant No. DMR-0213805) for support.

-
- [1] C. Ghidaglia, L. de Arcangelis, J. Hinch, and E. Guazzelli, *Phys. Rev. E* **53**, R3028 (1996).
 - [2] R. Narayan, J. Coury, J. Masliyah, and M. Gray, *Ind. Eng. Chem. Res.* **36**, 4620 (1997).
 - [3] S. Hong, R. Faibish, and M. Elimelech, *J. Colloid Interface Sci.* **196**, 267 (1997).
 - [4] Y. N. Xia and G. M. Whitesides, *Annu. Rev. Mater. Sci.* **28**, 153 (1998).
 - [5] T. Squires and S. Quake, *Rev. Mod. Phys.* **77**, 977 (2005).
 - [6] M. A. Unger, H.-P. Chou, T. Thorsen, A. Scherer, and S. R. Quake, *Science* **288**, 113 (2000).
 - [7] G. H. Goldsztein and J. C. Santamarina, *Appl. Phys. Lett.* **85**, 4535 (2004).
 - [8] K. V. Sharp (unpublished).
 - [9] W. B. Russel, D. A. Saville, and W. R. Schowalter, *Colloidal Dispersions* (Cambridge University Press, Cambridge, England, 1989).
 - [10] L. A. Spielman, *Annu. Rev. Fluid Mech.* **9**, 297 (1977).